Atmospheric Research 167 (2016) 196–207

Contents lists available at ScienceDirect

Atmospheric Research

journal homepage: www.elsevier.com/locate/atmos

Sensitivity of WRF short-term forecasts to different soil moisture initializations from the GLDAS database over South America in March 2009

María E. Dillon [a,b], Estela A. Collini [a,c], Lorena J. Ferreira [a]

[a] Servicio Meteorológico Nacional, Argentina
[b] Consejo Nacional de Investigaciones Científicas y Técnicas, Argentina
[c] Servicio de Hidrografía Naval, Argentina

ARTICLE INFO

Article history:
Received 23 January 2015
Received in revised form 15 July 2015
Accepted 20 July 2015
Available online 8 August 2015

Keywords:
Soil moisture initialization
Land Surface Models
Numerical Weather Prediction
Precipitation
Atmospheric Water Balance
South America

ABSTRACT

In Numerical Weather Prediction models it is essential to properly describe both the atmosphere and the surface initial conditions. With respect to the last, a major issue is the difficulty to attain a correct representation of soil moisture due to the lack of a measurement network established. This fact is crucial in South America. One alternative is the information given by the Land Surface Models (LSM), for example those provided by the Global Land Data Assimilation System (GLDAS).

Our main concern is to investigate the sensitivity of short-term numerical weather prediction to soil moisture initializations. The analysis is focused in precipitation mainly to the second forecast day, and other variables related to the atmospheric water balance. To accomplish this, we perform five experiments including some of the GLDAS databases (NOAH, VIC and MOSAIC) in the initialization of the Weather Research and Forecasting (WRF) model, during a test period of one month (March 2009). An initial field normalization procedure using one of the soil models as reference is also evaluated.

We show that the ambiguity of the soil models, given by their spatial and temporal variability as well as the forcing atmospheric fields, is transferred to the weather prediction model coupling, all over the month considered. Particularly, we show that the normalized percentage bias (NBIAS) of daily precipitation calculated for the second forecast day does not present well-defined patterns of over or underestimations: all the experiments show a wide range of variation. With respect to the normalized root mean square error (NRMSE) calculated for the same variable, we find that the values are generally low. In addition, the mean values of each statistic measure (NBIAS, BIAS, NRMSE and RMSE) do not show significant differences among the experiments (at 99% of significance). Nonetheless, it was shown that using the MOSAIC LSM for the initial conditions leads to minor NRMSE and RMSE maximums. Finally, while analyzing both moisture fluxes and precipitable water at different periods of the month, we find sensitive areas where the impact is mostly important, as Southeastern South America, central Argentina and Northeastern Brazil.

1. Introduction

It is well known that in order to achieve better results in short-term numerical weather predictions, the initial conditions must be improved. Not only an appropriate description of the atmosphere is essential, but also an adequate representation of the soil state. Many authors have shown the existence of land – atmosphere interactions over different parts of the world (de Goncalves et al., 2006; Betts, 2009; Sörensson et al., 2010; Seneviratne et al., 2010; Dirmeyer et al., 2012; Ferguson et al., 2012; Santanello et al., 2013; Zaitchik et al., 2013; Pathirana et al., 2014; Hirsch et al., 2014; among others). Both Eltahir (1998) and Pal and Eltahir (2003) proposed a positive feedback between wet soil moisture conditions and precipitation, through the enhancement of boundary layer moist static energy. Koster et al. (2004) analyzed the land atmosphere coupling strength during the boreal summer using the results of the Global Land – Atmosphere Coupling Experiment (GLACE), which yielded a multimodel average global distribution of the land-atmosphere coupling strength, with the aim of eliminating much of the undesired individual model dependence. This study showed hot spots of the land-atmosphere coupling in different regions of the world, addressing the local impact of soil moisture in precipitation, mainly in the transition zones between dry and wet climates.

Collini et al. (2008) studied the feedbacks between soil moisture and precipitation during the early stages of the South American monsoon, using the regional Eta model, and found a decrease of precipitation as an outcome of the initial soil moisture reduction. In the analysis carried out by Dirmeyer et al. (2009) from datasets containing both observations and numerical model results, the authors showed that the soil

http://dx.doi.org/10.1016/j.atmosres.2015.07.022
0169-8095/

moisture memory lasts less than 15 days over some regions of South America during the austral summer. This article motivated Saulo et al. (2010), who selected a particular case study to analyze the impact of the coupling between land and atmosphere in short to medium – range predictability over Southeastern South America (SESA). In fact, they found that more soil wetness enhances the convective available potential energy (CAPE) and in consequence it increases precipitation, and vice versa.

More recently, interactions between soil moisture and precipitation were evaluated by Ruscica et al. (2014) analyzing the coupling of soil moisture with surface and boundary layer variables, selecting subregions at SESA based on the soil moisture and evapotranspiration coupling and the mean intensity of precipitation.

Taking into account this evidence, an appropriate initialization of soil conditions, particularly of soil moisture, in a Numerical Weather Prediction (NWP) model would have a positive impact in the short-term forecasts quality.

The main issue is the difficulty to attain a correct representation of the soil moisture, particularly over SESA, which is our region of interest. Generally, soil moisture data is collected at few locations and for a short period of time: there is not an institutional gauging network established (Spennemann, 2010). Most of the data is obtained during field campaigns which are regional and sporadic, so it can not be used to initialize NWP models on regular basis. An alternative would be to use satellite estimations in order to have a wide coverage, both spatial and temporal, but those estimations generally correspond to the superficial soil moisture from a layer of a few centimeters depth. For example, this is the case of the data derived from the passive radiometer AMSR-E on board of EOS-Aqua satellite, which has 2 algorithms to obtain the soil moisture retrieval: the one developed by NSIDC – NASA (National Snow and Ice Data Center and NASA) (Njoku, 1999) and the other generated by VUA – NASA (Vrije Universiteit Ámsterdam and NASA) (Owe et al., 2008). However, it has been demonstrated in various regions that the soil dynamics explained by each of the algorithms are different (Rudiger et al., 2009; Draper et al., 2009; Dillon et al., 2012), leading to uncertainties about which is the best estimation.

On the other hand, there are many uncoupled soil models developed that are forced by atmospheric conditions, fixing the shortcoming of the soil variables data. One of the most important projects is the Global Land Data Assimilation System (GLDAS) composed of four models with different characteristics (Rodell et al., 2004). Monthly and three hourly fields are available from distinct depths from the CLM (Community Land Model), Mosaic, NOAH and VIC (Variable Infiltration Capacity) models. Particularly, the soil moisture obtained from these databases has been used by several authors for atmospheric and hydroclimatic studies (Zhang et al., 2008; Liu et al., 2009; Spennemann, 2010; Ferreira et al., 2011; Dillon et al., 2012; among others).

In the present work, our main concern is to investigate through a sensitivity study, how is the impact of the soil moisture initialization over the short-term numerical weather prediction in South America, using the Weather Research and Forecasting (WRF) model. To accomplish this, we perform five experiments including some of the GLDAS databases in the initialization of the WRF, where we analyze the impact of the different initializations on the precipitation forecasts and the vertically integrated moisture fluxes, among other variables. An initial field normalization procedure (Koster et al., 2009) using the NOAH/GLDAS soil model as a reference is also evaluated. The data and methodology are described in Section 2, while the results are presented in Section 3. Finally, the remarks are summarized in Section 4.

2. Methodology

Our study is concentrated on March 2009. The selection of this particular month is related to the beginning of the precipitation over SESA, after an intense drought that has been affecting this region for more than a year. La Niña event was established at the last quarter of 2007 and prevailed during 2008, favoring the reduction of precipitation over La Plata Basin (http://www.atmos.umd.edu/~berbery/lpb/). Anomalies up to minus 60 percent of the annual mean precipitation were registered in this region. It was qualified as the worst drought in the last 65 years (Peterson and Baringer, 2009; Arndt et al., 2010).

In order to assess the interaction between the atmosphere and the soil moisture during this period, we employed the Advanced Research Weather (ARW) core, from **WRF** model version 3.1.1, which runs experimentally at the National Meteorological Service of Argentina since 2010, in an automatic but non operational way (Collini et al., 2011). Its spatial resolution is 24 km in the horizontal and 38 levels in the vertical (50 hPa model top), in a domain including South America and the adjacent oceans. Some of the parameterizations chosen are: the Rapid Radiative Transfer Model (RRTM) for long wave radiation (Mlawer et al., 1997) and the Dudhia scheme for the short wave one (Dudhia, 1989); the Betts – Miller – Janjic scheme for cumulus parameterization (Betts and Miller, 1986; Janjic, 1994); the Eta microphysics scheme (Zhao and Carr, 1997); the similarity Eta parameterization for the surface layer (Monin and Obukhov, 1954; Zilitinkevich, 1995); the Mellor – Yamada – Janjic scheme for the boundary layer (Janjic, 1990, 1996, 2002; Mellor and Yamada, 1982). In addition, the NOAH model was chosen to be in accordance with the land surface model (LSM) coupled in the Global Forecasting System (**GFS**), at the National Centers for Environmental Prediction (NCEP), whose analysis and 3 hourly forecasts of 1° x 1° latitude-longitude resolution were used as initial and boundary conditions respectively for the WRF. The NOAH has 4 soil layers: 0 – 0.1 m, 0.1 – 0.4 m, 0.4 – 1 m and 1 – 2 m (Chen and Dudhia, 2001).

We designed five sets of forecasts to carry out sensitivity studies, using some of the GLDAS version 1 uncoupled soil models (http://disc.sci.gsfc.nasa.gov/services/grads-gds/gldas) as initial soil moisture conditions. These datasets are forced by a combination of the Global Data Assimilation System (GDAS) analysis and the Climate Prediction Center Merged Analysis of precipitation (CMAP), and therefore, they receive information from surface and satellite observations (Rodell et al., 2004). In the present article three of the models are used, with a spatial resolution of 1°x1°: **Mosaic** (Koster and Suarez, 1996), which is based on the Simple Biosphere (SiB) model and has 3 layers of depth: 0 – 0.02 m, 0.02 – 1.5 m and 1.5 – 3.5 m; the **NOAH** model (Chen et al., 1997; Koren et al., 1999), mentioned above; and the **VIC** (Liang et al., 1994; Liang et al., 1996) model, which divides the soil into 3 layers: 0 – 0.1 m, 0.1 – 1.6 m and 1.6 – 1.9 m.

Each set of forecasts consists of thirty-one 2-day forecasts initialized at 12 UTC on each day of March 2009, using a WRF non – hydrostatic

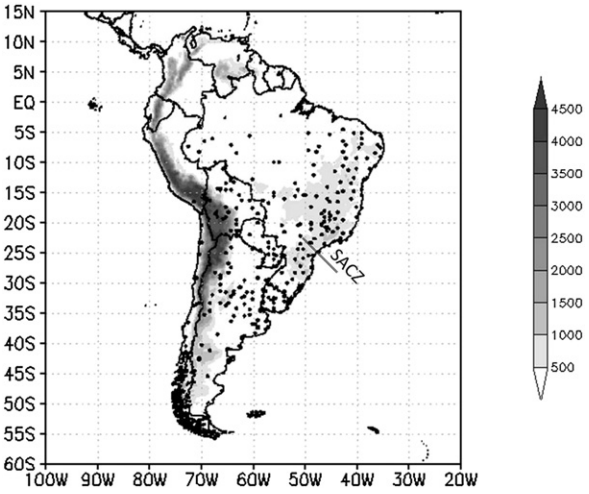

Fig. 1. Meteorological stations used in the precipitation forecast verification (dots), and the WRF topography [m] (shaded) in the full domain used in the simulations. The full line denotes the South American Convergence Zone (SACZ).

Table 1
The soil models used to initialize the soil moisture of each experiment.

	Exp. A (Control)	Exp. B	Exp. C	Exp. D	Exp. E
Initialized with	NOAH/GFS	NOAH/GLDAS	MOSAIC/GLDAS	VIC/GLDAS	MOSAIC/normalized

configuration over the domain presented in Fig. 1. In Table 1 these experiments are summarized. We define the experiment initialized with the NOAH from the GFS as the control run (Exp. A), because this LSM is the one used frequently for operational settings. The Exp. B corresponds to the initialization with the NOAH from the GLDAS dataset, while experiments C and D are the ones where the Mosaic and VIC models from the GLDAS dataset were used for the initialization, respectively. As the number of soil layers from these models is different, a linear interpolation to the four NOAH soil depths was performed. Finally, the Exp. E refers to a normalization applied by Dirmeyer et al. (2004) and Koster et al. (2009) to climatic scales, to compare soil moisture from several models. These authors showed that each model has a special dynamical range, so that a wet (dry) state of one model is not necessarily a wet (dry) state of another one, and therefore, it would be adequate to use one model as a reference for the others. In a synoptic scale, Dillon et al. (2011) applied a normalization based on this hypothesis in a case study.

The authors present a normalization for the Mosaic model (Exp. E) using the NOAH/GLDAS model as the reference. Following that methodology the mean values of the soil moisture from the MOSAIC/GLDAS ($\overline{x_m}$) and NOAH/GLDAS ($\overline{x_n}$) models for March between the years 2000 and 2009 were first calculated, and then the standard deviations of March 2009 with respect to those means were estimated (σ_m and σ_n). It is worth to say that this 10-years period was selected in order to have a homogeneous dataset from GLDAS, as the previous years different databases were used to initialize the soil models (Rui, 2011).

Finally this normalization procedure was applied for each day using the Equation (1), which is analogous to Equation 2 from Koster et al. (2009).

$$x_n = (x_m - \overline{x}_m)\frac{\sigma_n}{\sigma_m} + \overline{x}_n \quad (1)$$

where x_m and x_n represents the soil moisture from the MOSAIC/GLDAS and the NOAH/GLDAS respectively, for a particular day. Therefore, the soil moisture of model "*m*" could be read consistently by the model "*n*", so that a dry (wet) state of the model "*m*" is translated to a dry (wet) state of the model "*n*".

The evaluation of the experiments' results is done either for all days in the month or for three periods, which correspond to a characterization of the synoptic features for the whole month carried out through the examination of the Climate Forecast System Reanalysis data base (CFSR, Saha et al., 2010). Focusing over the south of the La Plata Basin, below 25°S, three periods can be considered: the first 12 days presented moderate precipitation; while from the 13th to the 23th of March there was neither precipitation in the area, nor presence of specific humidity values higher than 0.01 $kgkg^{-1}$ in the low levels of the atmosphere (mostly near the surface); and the last part of the month was also characterized by non precipitation, although the moisture at low levels started to increase.

The daily precipitation accumulated between the 24 and 48-hour forecasts was calculated at the 165 meteorological stations shown in Fig. 1, obtained from the GTS network. Namely, as the major data availability is from the entire day precipitation, which stands from 12 UTC to 12 UTC, and considering that the model has 6 hours of spin-up approximately, we evaluate the 24-hour precipitation accumulated during the second day of the set of forecasts (second forecast day). In order to obtain statistical results, the normalized percentage bias (NBIAS) (Su et al., 2008) and the normalized root mean square error (NRMSE) (Yilmaz et al., 2005) were calculated for the whole month, in addition to the traditional BIAS and RMSE absolute measures. With the normalized statistics, one can become independent from the precipitation values of each station, but taking into account that little amounts of precipitation would lead to huge values of the normalized statistics. With respect to the NBIAS, positive (negative) values correspond to overestimations (underestimations), just like the traditional BIAS. With respect to the NRMSE, values near to zero indicate low errors, just like the traditional RMSE too.

Moreover, the changes in the soil moisture initialization not only impact on the precipitation but also they alter the moisture transport among regions (Pal and Eltahir, 2003; Collini et al., 2008; Seth and Rojas, 2003; Wei and Dirmeyer, 2012), as can be inferred from the model patterns of the moisture flux. To obtain these patterns, here we calculate the vertically integrated moisture flux for each of the experiments over the whole WRF-ARW domain, performing calculations with schemes that are consistent with those used by the model. The anomalies calculated in relation to the control run (Exp. A) show the regional dependence of the moisture flux patterns, which will be illustrated in the next section.

Also, the response of the column-integrated total precipitable water content (PWAT) (Berbery and Rasmusson, 1999) to the different initializations over the region of study will help to understand the effect on the atmospheric water balance. This is particularly important over Amazonia, where the atmosphere is typically moist at all levels leading to a huge moisture content over land, which is comparable to or larger than over the adjoining oceans (Berbery and Collini, 2000) and where there are signs of land–atmosphere feedback throughout most of the year (Dirmeyer et al., 2009; Grimm et al., 2007).

3. Results

In this Section we discuss the results from the different experiments, at first presenting a deep insight of the different fields of soil moisture and their impact on the forecast of precipitation, and then showing a comparison between some vertically integrated variables forecast obtained from diverse initial soil states.

3.1. Soil moisture and its impact on precipitation

The soil layer that interacts mostly with the atmosphere corresponds to the first centimeters of depth. Hillel (1998) stated that "*the soil's surface zone is indicative of the entire interaction between the land surface and the atmosphere, since it regulates such processes as the exchange of energy*". Likewise, Sanchéz-Mejía (2013) showed the influence on the surface energy budget and Planetary Boundary Layer characteristics of a layer of 20 cm depth, using a two soil moisture layer conceptual model where this one was defined at reach of atmospheric demand.

Therefore, the volumetric soil moisture of the 10 centimeters superficial layer averaged for March 2009 for experiments A, B, C, D and E, is shown in Fig. 2. The average was calculated for 12 UTC, the initial time of the forecasts.

The five experiments show the driest region over Chile, Argentina and the northeast of Brazil, and the most humid region over the Amazon forest, although the magnitude of soil moisture varies among them. La Plata Basin, which includes the northeast of Argentina, Paraguay, the south of Brazil and Uruguay, is a transition zone between wet and dry climates and is the area that presents more uncertainties. The Exp. C

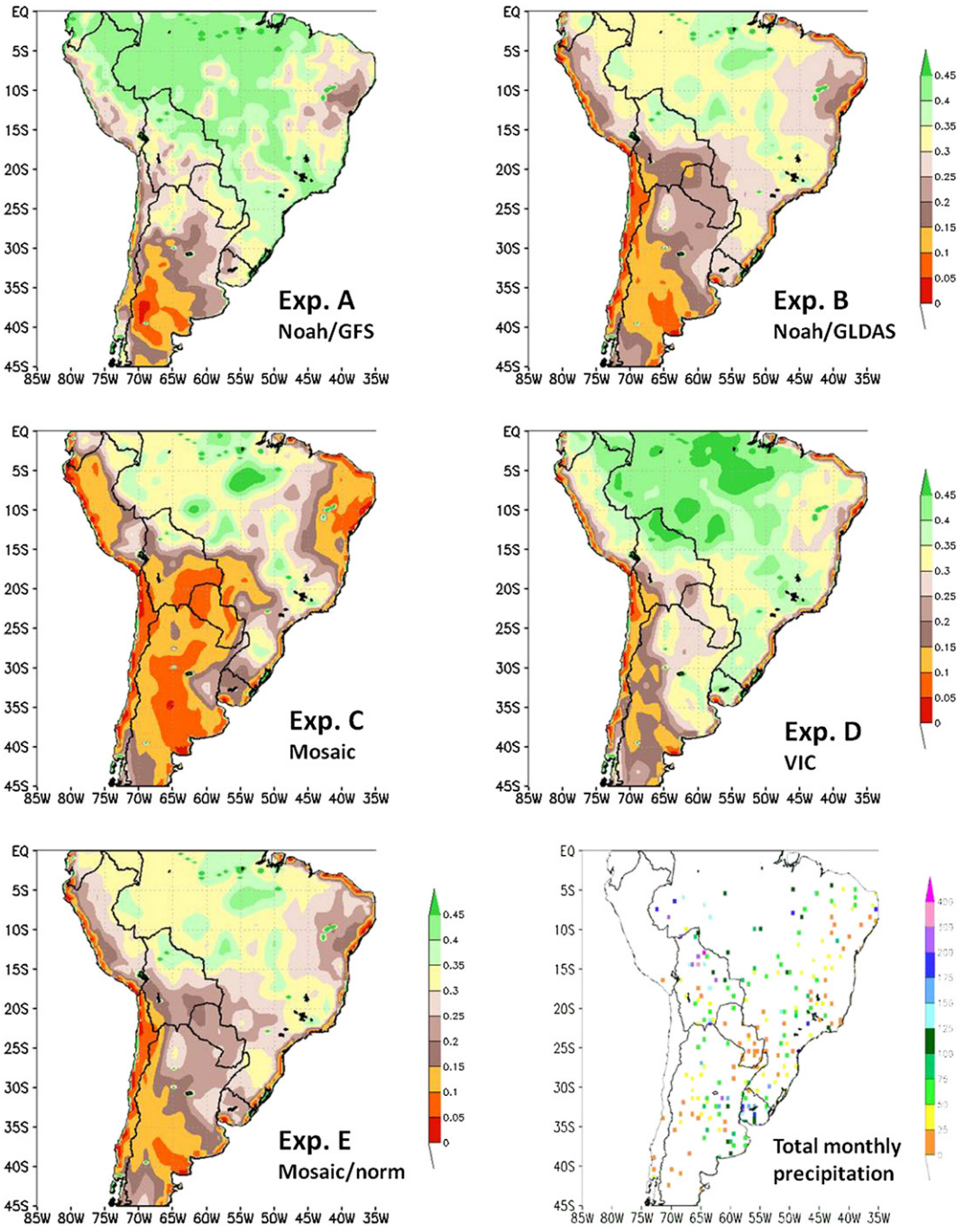

Fig. 2. Monthly averaged volumetric soil moisture of the 0-0.1 m layer [m^3m^{-3}] for March 2009. Upper panel: Exp. A (left) and Exp. B (right); middle panel: idem for Exp. C (left) and Exp. D (right); lower panel: idem for Exp. E (left), and total monthly observed precipitation [mm] (right). The averages were calculated for 12 UTC, the initial time of the forecasts.

exhibits the driest field of soil moisture while the Exp. D shows the wettest one, showing a strong gradient between 0.15 and 0.3 m^3m^{-3} in the transitional area.

The normalization described in Section 2 (Exp. E) shows an averaged soil moisture field similar to, but drier than the NOAH/GLDAS, due to the influence of the MOSAIC/GLDAS field. This is an expected result as the purpose of the methodology was to translate one model in terms of the other.

The experiments A and B show different results, even though they correspond to an initialization with the same Land Surface Model: the NOAH. Actually, Exp. A is wetter than Exp. B over almost the entire domain. These differences are due to the distinct meteorological forcing fields in each run of the NOAH LSM, as it was described in the previous Section. Moreover, the initial soil moisture of Exp. A was obtained from a coupled system in which there is a feedback between the atmospheric and soil conditions, in contrast to the one of Exp. B which was produced by an uncoupled soil model.

The monthly precipitation in the meteorological stations analyzed for March of 2009 is shown in the lower panel of Fig. 2. The maximum values were registered over Bolivia and the west of Brazil while the other stations showed values below 100 mm, except for some stations from the central part of Argentina and Uruguay. Generally, the areas with greater amount of precipitation agree with the wetter soils in the five experiments, as we can see in the other panels of the Figure.

Unfortunately, at the present time there is not a South American data base of soil moisture *in situ* measurements, although many efforts have

been done by the Community during the last years (Dorigo et al., 2011). Particularly, in Argentina a joint project between the CONAE (National Space Activities Commission) and the National Meteorological Service is carried out with the aim of installing soil sensors in the surface meteorological stations across the country (Dillon et al., 2012). We can also mention other efforts made in the region as the Joint Assessment of Soil Moisture Indicators (JASMIN Project, Berbery et al., 2014) for Southeastern South America.

Therefore, nowadays we are not able to conclude which of the experiments exhibit the best representation of the soil moisture field, as we do not have an observed field. In this sense, we evaluate the impact of the initial soil state in the forecast of precipitation.

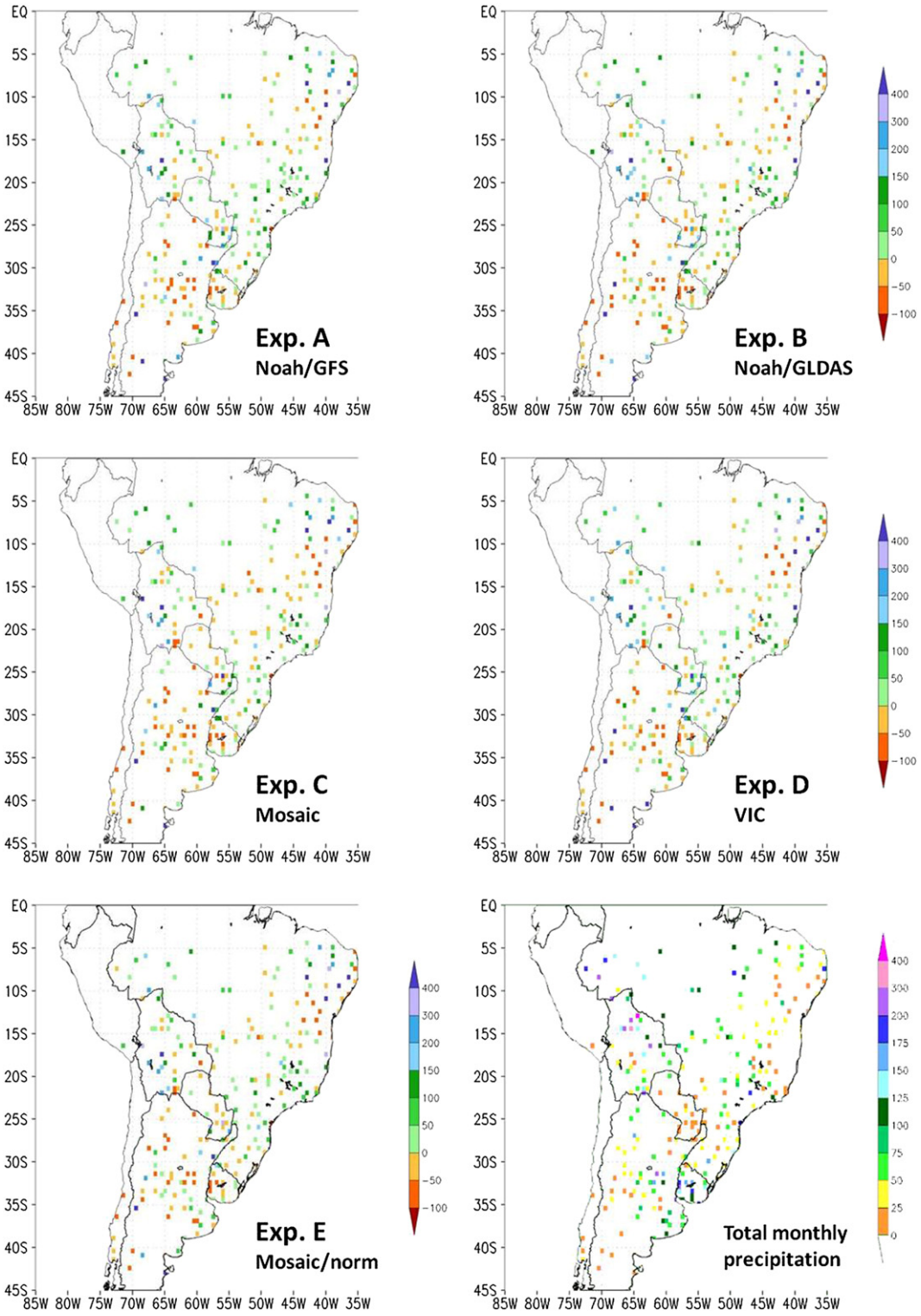

Fig. 3. Upper panel: Normalized percentage bias (NBIAS) of daily precipitation forecasted for 48-hour for March 2009: Exp. A (left) and Exp. B (right); middle panel: idem for Exp. C (left) and Exp. D (right); lower panel: idem for Exp. E (left), and total monthly observed precipitation [mm] (right).

The normalized percentage bias (NBIAS) of daily precipitation calculated for the second forecast day does not present well-defined patterns of over or underestimations: all the experiments show a wide range of variation (Fig. 3). However, over the land portion of the South American Convergence Zone (SACZ) region an overestimation of precipitation is detected in most of the stations

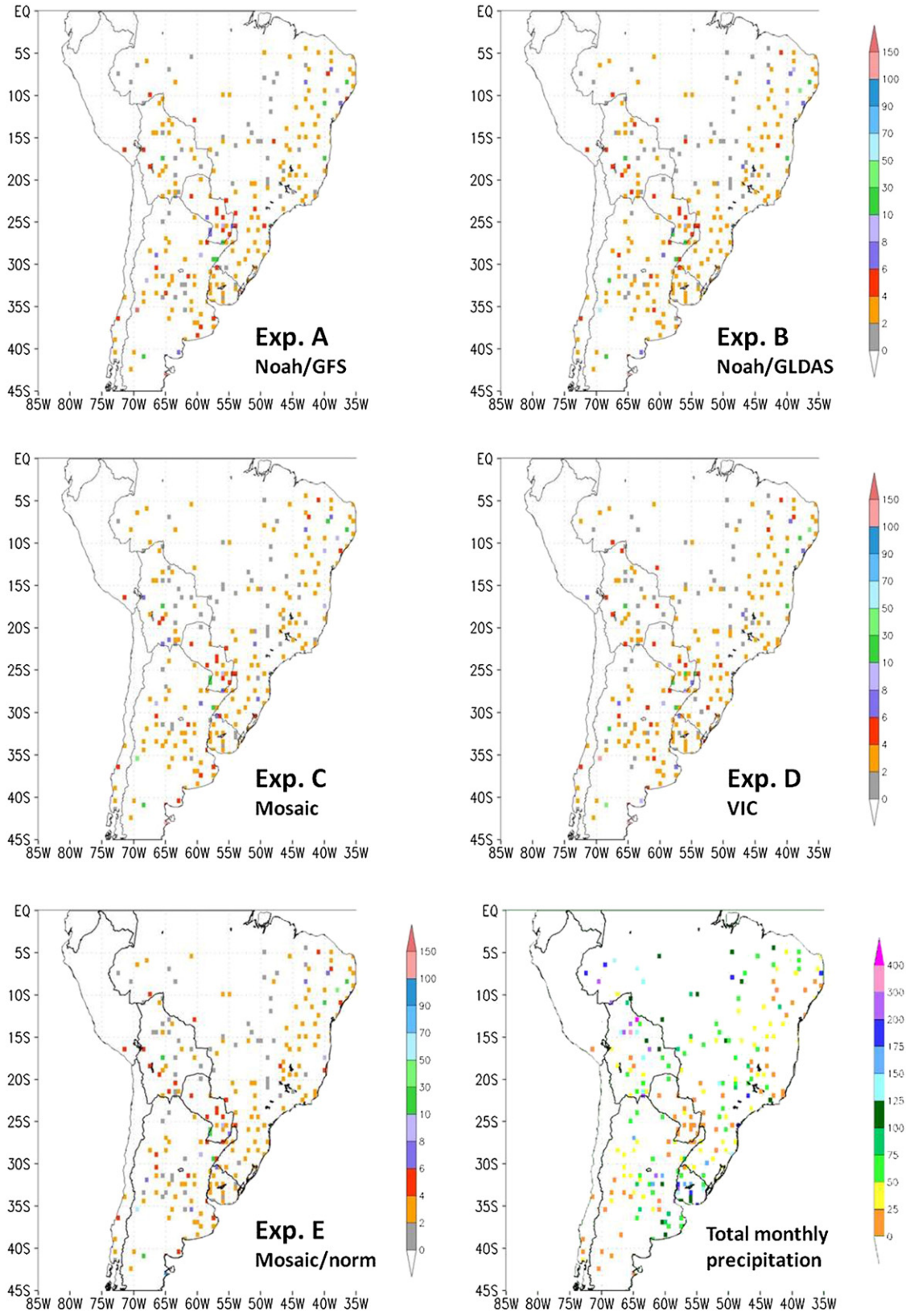

Fig. 4. Upper panel: Normalized root mean square error (NRMSE) of daily precipitation forecasted for 48-hour for March 2009: Exp. A (left) and Exp. B (right); middle panel: idem for Exp. C (left) and Exp. D (right); lower panel: idem for Exp. E (left), and total monthly observed precipitation [mm] (right).

Table 2
Maximum, mean and minimum values of the Normalized Bias and RMSE, for each experiment, calculated for the precipitation second forecast day (see text for details). The best score at each statistical measure is in bold.

	Exp. A	Exp. B	Exp. C	Exp. D	Exp. E
NBIAS max	830.5	1283.37	926.8	**820.5**	1250.5
NBIAS mean	44.69	38.42	**33.61**	48.8	37.19
NBIAS min	-91.95	-92.46	-90.14	**-86.59**	-91.31
NRMSE max	23.54	46.09	**19.64**	25.67	44.07
NRMSE mean	3.37	3.41	**3.34**	3.41	3.39
NRMSE min	0.9	0.95	0.9	**0.89**	0.92

for all the experiments, which agree with the results obtained in a case study by Saulo et al. (2010).

In Fig. 4 the normalized root mean square error (NRMSE) of the second forecast day precipitation is shown for all the experiments. Generally low values (between 0 and 4) are found, with the exception of some isolated stations from Brazil, Argentina and Paraguay that show higher values in the five cases. However, these stations correspond to a monthly accumulated precipitation under 5 mm, which may explain the large values of the NRMSE.

In order to summarize these results, Table 2 presents the minimum, maximum and mean values of both normalized statistics, for each experiment considering the stations where the monthly accumulated precipitation was more than 5 mm. Looking at the mean values of NBIAS, the one that corresponds to Exp. A is greater than the one in Exp. B, in agreement with the fact that the averaged soil moisture of the NOAH/GFS is wetter than that of the NOAH/GLDAS (Fig. 2). Moreover, Exp. D shows the highest mean value of NBIAS probably due to its wettest soil moisture initial conditions. However, neither the Exp. B, C, D nor E is significantly different from the Exp. A considering the NBIAS mean (at 99% of significance). With respect to the maximum NBIAS, the large amounts correspond to isolated stations with a little amount of monthly precipitation (less than 15 mm) and this is why when the normalization and percentage are taken the value increase significantly. The NRMSE values are very similar among the five experiments, and in fact although the Exp. C shows the lower mean value, it is not significantly distinct from the one from Exp. A (at 99% of significance).

In addition, Table 3 shows the minimum, maximum and mean values of the absolute statistics RMSE and BIAS, calculated for the precipitation of the second forecast day too. The values of the BIAS varies between about -9 and 20 mm/day presenting a similar range to the one shown by Ruiz et al. (2010), who found bias from -10 to 15 mm/day in the same region, through a change in WRF parameterizations during one summer case. Both BIAS and RMSE values do not differ so much among the experiments: particularly their mean values do not differ significantly (at 99% of significance).

Using the information from both Tables 2 and 3 it seems that the "best" scores analyzing the precipitation forecast are from Exp. C; i.e. the set of forecasts initialized with the Mosaic soil moisture is the one which showed the minor NRMSE and RMSE maximums, and the minor NBIAS, NRMSE and BIAS means (although these are not significantly different from the Exp. A).

Table 3
Maximum, mean and minimum values of the absolute Bias and RMSE, for each experiment, calculated for the precipitation second forecast day (see text for details). The best score at each statistical measure is in bold.

	Exp. A	Exp. B	Exp. C	Exp. D	Exp. E
BIAS max	19.79	19.33	**18.15**	20.17	20.03
BIAS mean	0.91	0.69	**0.53**	0.99	0.67
BIAS min	-8.61	-9.08	-9.32	**-8.15**	-8.56
RMSE max	8.77	8.86	**8.02**	9.07	9.09
RMSE mean	2.18	2.19	2.18	2.19	**2.17**
RMSE min	0.18	0.17	0.14	**0.13**	**0.13**

In the following paragraphs, the impact of the different initializations on the forecasts of vertical moisture fluxes and precipitable water is discussed.

3.2. Impact on vertically integrated variables forecast

The soil moisture initialization can lead to changes in the precipitation forecasts, as we have seen in our experiments (Section 3.1) and as many others authors have shown for regions all over the world (Eltahir, 1998; Betts and Viterbo, 2005; among others). Koster et al. (2009) stated that the single soil moisture variable, at a given vertical level in a land surface model, must reflect more than the average soil moisture across about 100 km. Also, it reflects somehow, the spatial variability of soil moisture and its effects on the surface energy and water fluxes.

In this Section we discuss the response of the column integrated precipitable water up to 300 hPa and the vertical moisture flux to the changes in the soil moisture initialization. Also, we show the effectiveness of the normalization procedure (Koster et al., 2009) even at regional and synoptic scales.

As a first step we show some features of the control experiment (Exp. A) in Fig. 5. The precipitable water content averaged for March 2009 considering the analysis time (12 UTC) shows values higher than 25 mm for the entire La Plata Basin (LPB). The moisture flux convergence (defined as positive values) has a dominating maximum over the Amazonas, and near-zero values over the LPB. Nevertheless, it is noteworthy that the vertically integrated moisture flux has a northerly component over SESA, bringing the Amazonian moisture into this region.

In the following figures, we analyze either the 24-hour or the 48-hour forecasts of different variables, for the three different periods defined on Section 2. For example, for the case of the first period, we consider the forecasts of the models initialized each day from 1st to 12th March.

From the Fig. 6 we can evaluate the impact of the MOSAIC/GLDAS, MOSAIC/normalized and NOAH/GLDAS initializations with respect to the NOAH/GFS initialization for the 24-hour forecast, averaged for the third period (24th – 31st March) when a maximum northerly flow at low levels occurs. Centered over the Amazon Basin and slightly over eastern Bolivia are the areas where the differences are found in all the experiments. For Exp. C, the anomalies strengthen all over the domain and the maxima are located at eastern Bolivia (120-140 kg m^{-1} s^{-1}). Particularly, over western Paraguay and northern Argentina, the anomalies of Exp. C (relative to Exp. A) do not appear in the experiments B and E.

Then, a consequence from the normalization procedure (Exp. E) is the reduction of the anomalies in values and domain of influence for both forecast periods (48-hour forecast results not shown). The normalization procedure produces a dryness of the soil layers and consequently the initialization using Normalized MOSAIC gives moisture convergence fields very close to the NOAH/GLDAS initialization (Fig. 6). These results demonstrate that the assertion of Koster et al. (2009) for global scale can be extended to regional scales, in the sense that if the soil moisture fields in two models are well known, a mapping could be derived that would allow the soil moisture variable from one model to be transformed and applied effectively in the other.

There is no large impact of the different initializations in the water vapor balance when the atmosphere is moist enough; instead it is thoroughly noted during the dry/almost dry periods. This agree with the latest findings by Angelini et al. (2011) who pointed out that the rain in Amazonia comes primarily from large-scale weather systems from the tropical Atlantic, that do not rely on local evaporation. Particularly, this circulation from the Atlantic Ocean and Northeast Brazil (NEB) towards the Amazonia region can be addressed with the moisture flux features of March 2009 (Fig. 5). Then, changes in the soil moisture field impacts slightly in this region.

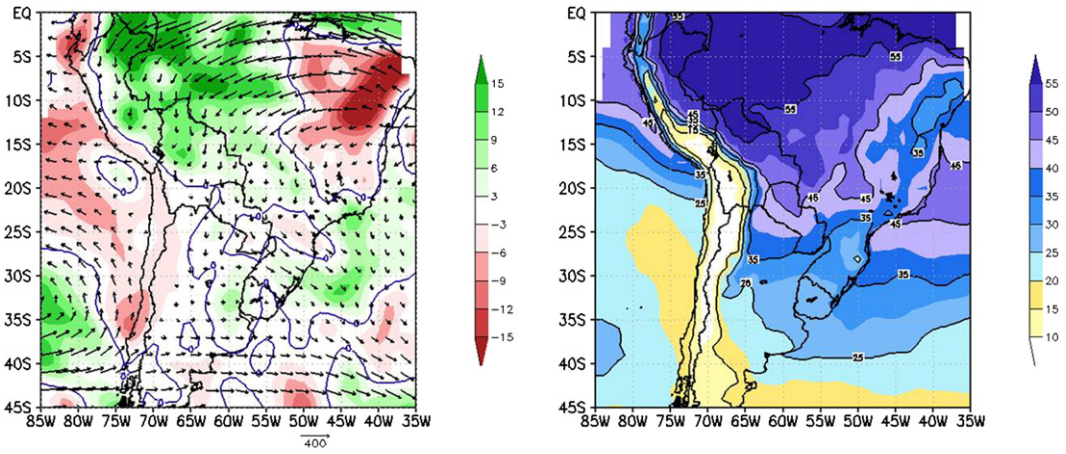

Fig. 5. Left panel: Monthly averaged vertically integrated moisture flux (vectors) [kg m^{-1} s^{-1}] and vertically integrated moisture flux convergence (shaded) [kg m^{-1} s^{-2}], where positive values correspond to convergence and negative values correspond to divergence, and zero is denoted with a contour. Right panel: Monthly averaged precipitable water [mm]. The average was calculated for 12 UTC, the initial time of the forecasts, for the Exp. A (Control) considering March 2009.

As it is evident from Fig. 2, the monthly averaged volumetric soil moisture for the five experiments shows a significant range of values, being the Exp. C the driest field and the Exp. D the wettest. For this reason we analyze the differences resulting from these two initializations of the soil moisture state during the second period (13th – 23rd March), which was characterized by lack of precipitation and low specific humidity in the lower troposphere. The spatial pattern of the soil moisture fields can lead to a horizontal gradient in atmospheric states, influencing circulation and vapor convergence (Miguez-Macho et al., 2008). To assess the impact for the maximum range of variation of the soil moisture initialization, we analyze the differences for precipitable water and vertically integrated moisture flux between the most humid and the driest of the soil models: VIC/GLDAS (Exp. D) and MOSAIC/GLDAS (Exp. C) respectively (Fig. 7).

In the case of the vertically integrated moisture flux, the discrepancies between the initializations mainly maximize in the tropical regions

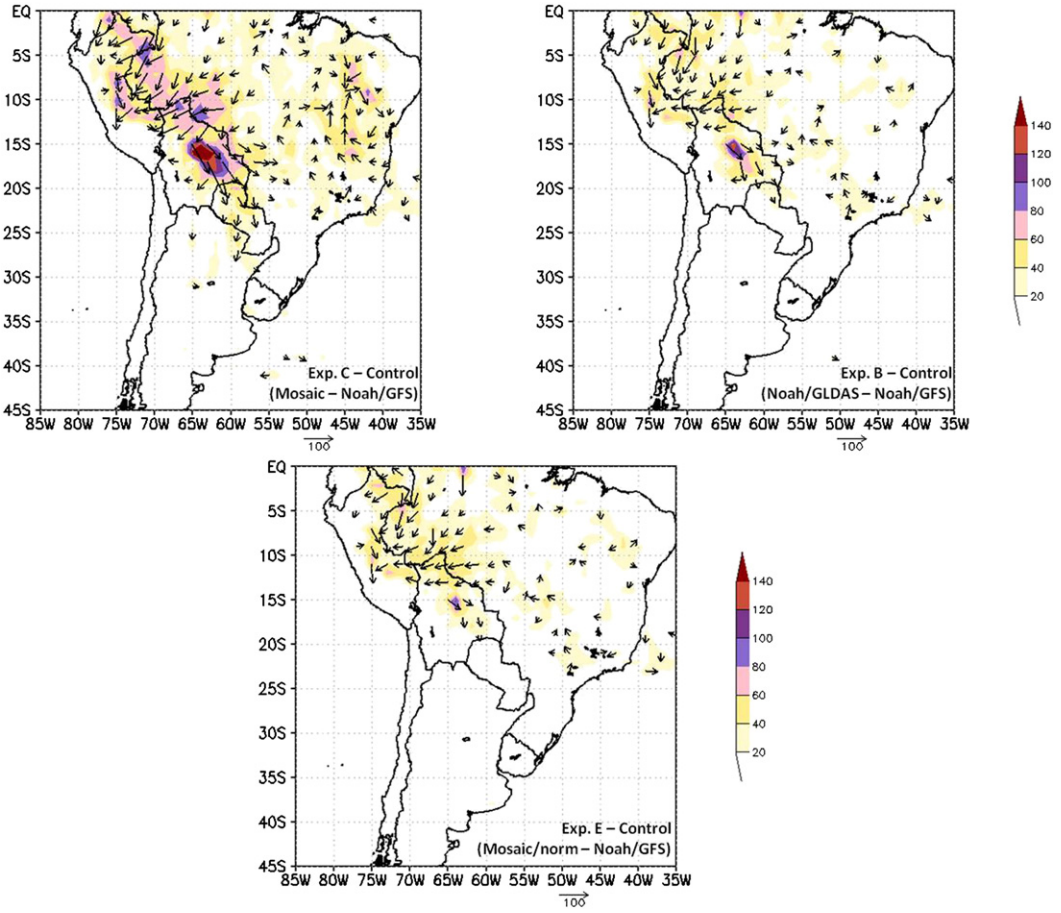

Fig. 6. 24-hour vertically integrated moisture flux forecast differences averaged for the period 24-31 March 2009: Exp. C – Exp. A (upper left panel); Exp. B – Exp. A (upper right panel); Exp. E – Exp. A (lower panel); [kg m^{-1} s^{-1}]. Shaded values correspond to the magnitude of the vectors.

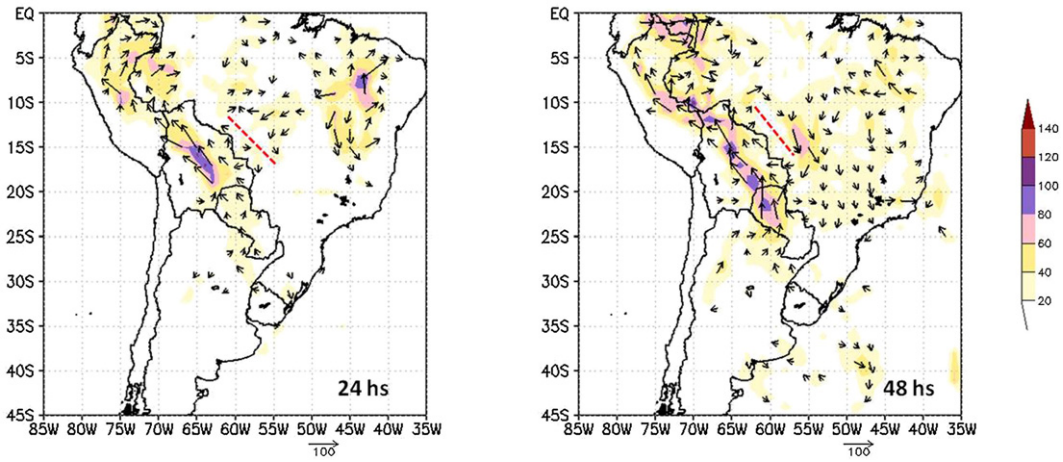

Fig. 7. Vertically integrated moisture flux differences (Exp. D – Exp. C) forecasted for 24-hour (left panel) and 48-hour (right panel), averaged for the period 13 – 23 March 2009; [kg m^{-1} s^{-1}]. Shaded values correspond to the magnitude of the vectors.

no matter which time period or forecast length is considered. The difference between both experiments to the west of the Brazilian border (see the red oblique line at Fig. 7) indicates that the Exp. D fluxes are stronger than the Exp. C ones, while to the east they look similar or weaker. There are scarce and weak differences over northern Argentina, but over the rest of the country the two experiments of the WRF model with different soil moisture initialization each, apparently behave similarly. In the particular case of the 48-hour forecasts the differences strengthen over the continental SACZ and are also transported to the Atlantic Ocean mainly south of 30°S.

In the Fig. 8 the differences between the precipitable water forecasted by experiments C and D, for 24 and 48-hour and averaged for each period, are shown. For the first period a similar pattern is found over NEB for both forecast intervals, but over more extended areas in the 48-hour one, showing largest values as of around -4 mm. During the second part of the month, there is again a maximum negative variation over NEB, as well as positive differences sparsely distributed over the Southeastern South America with increasing values from the 24 to the 48-hour forecast. The northeastern region of Brazil is semiarid with a single season from February to May that provides 70% of the annual rains (Seth and Rojas, 2003). The NEB shows values of precipitable water that depend on the topography (being low at the elevations and large over the plains neighboring the Equator) and partly on the vegetation cover (Cavalcanti et al., 2002). The different approach to these regional characteristics in the GLDAS soil models could produce the largest anomalies shown. It should be noted that in the second and the third period, large differences (~4 mm) can be seen along and east of the Andes south of 25° S. These differences arise from larger values of precipitable water in the Exp. D than in the Exp.C.

Apparently, both experiments of the WRF model that differ in the soil moisture initialization agree overall in the Amazon Basin, where largest values of precipitable water exceeding 50 mm can be found (not shown). The initial soil moisture used in Exp. C and Exp. D are able to well describe the nearly moist-adiabatic lapse rate which characterizes the Amazon basin troposphere.

The comparison among the PWAT forecast differences for the three periods, reinforces the fact that the influence of the initialization is stronger for the driest atmospheres. For the dry periods, the 48-hour PWAT forecast differences exceed those of the 24-hour forecasts, showing that the changes in the initial conditions affect all the length of the forecast. Particularly, for the second period and over Argentina to the East of the Andes between 25°S and 35°S, differences of around 4 mm are found in the 48-hour forecast compared with the 2 mm of the 24-hour one.

East of the Central Andes, from the tropics to Northern Argentina, an elongated moisture convergence for the period from 13th to 23th March pattern is found. In that region, no differences were detected in PWAT. Meanwhile, for the third period of March, both models agree in a pattern of moisture coming from the Intertropical Convergence Zone (ITCZ) and transported throughout the middle of Brazil reaching the SACZ (not shown) where, the Exp. D shows larger PWAT values than the Exp. C. especially on the 48-hour forecast period. Moreover, the Exp. C PWAT values are greater than those of Exp. D over Northwestern and Northeastern Argentina, and the opposite occurs over the East and Central Argentina.

Generally, the analysis of some variables related to the atmospheric water balance as well as the range between the driest and wetest models show that the impact of the interaction between the soil state and the atmosphere depends mostly on the regional and sub-regional features. A more detailed research should be addressed focusing in the split of the region into sub-regions, taking into account the diversity in terms of land use, vegetation, hydrology, among other aspects.

4. Conclusions

Our main concern is to analyze the impact of soil moisture initializations in precipitation forecast and other variables related to the atmospheric water balance, using different outputs coming from Land Surface Models, for March 2009. We showed that the ambiguity of the soil models, given by their spatial and temporal variability as well as the forcing atmospheric fields, was transferred to the weather prediction model coupling.

With respect to the precipitation forecasts, in the case of the NOAH/GFS as LSM initial condition, the results were in close agreement with the observations: both the absolute and normalized RMSE means exhibited values less than 3.5. Likewise, when we compared the mean values of all the statistics measures obtained from the experiments using the NOAH/GLDAS, MOSAIC/GLDAS, VIC/GLDAS or MOSAIC/normalized as LSM initial condition, with the one of NOAH/GFS, no significant differences in the predictions were found (at 99% of significance). Nonetheless, it was shown that using the MOSAIC/GLDAS LSM for the initial conditions leads to minor NRMSE and RMSE maximums.

It is worth to say that these results verify for a particular month, and therefore, they are not a definitive asseveration. Thus, the experiments should be generated during longer periods of time in order to achieve a more consistent conclusion. Also, a denser precipitation network acquired within a joint effort for reaching inter-institutional operability among different networks should provide a more accurate measure of error for evaluation purposes. These aspects will be future research goals.

While analyzing both moisture fluxes and PWAT at different periods of the month, we found sensitive areas where the impact was mostly

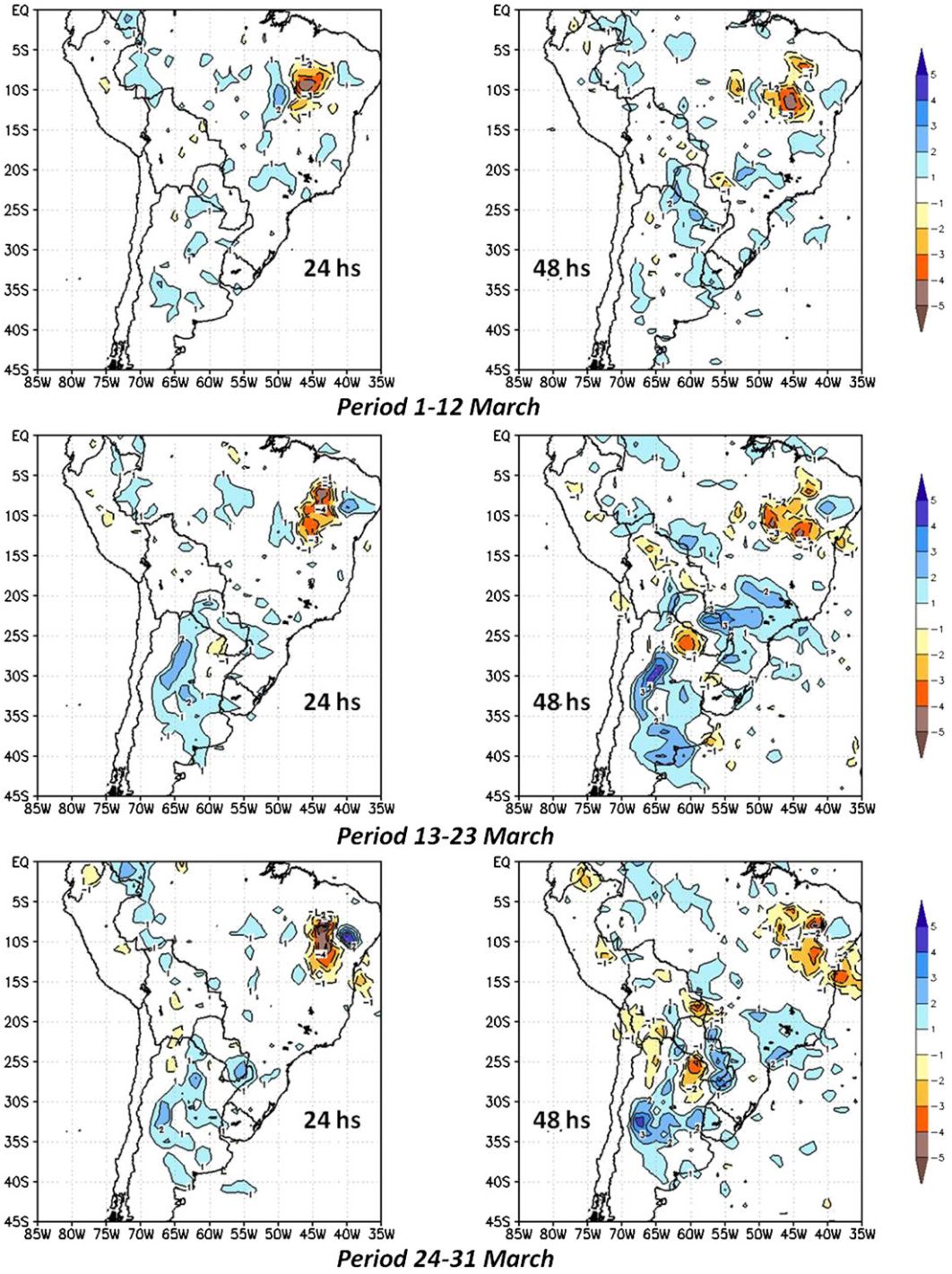

Fig. 8. Averaged Precipitable water differences (Exp. D – Exp. C) forecasted for 24-hour (left panel) and 48-hour (right panel) for the three periods indicated: 1 – 12 March 2009 (upper panel); 13 – 23 March 2009 (middle panel); 24 – 31 March 2009 (lower panel); [mm].

important, as Southeastern South America, Central Argentina and Northeastern Brazil.

In the last few years, there was a rapid development of the sophisticated LSM schemes, and a rapid expansion in their applications in atmospheric, hydrological, and ecological modeling. On the contrary, there is a lack of large temporal and widespread soil moisture observations datasets to enable to generate a consolidated dataset for extensive evaluation purposes. Joint efforts should continue and increase in these directions, LSM schemes and *in situ* datasets, in order to enrich the knowledge on the land-atmosphere interaction, which is a very important issue. Recently, Dirmeyer et al. (2013) stated that the land-atmosphere coupling is expected to be reinforced in the future throughout most of the globe, meaning a greater control by soil moisture variations on surface fluxes and the lower troposphere.

Acknowledgements

The WRF/ARW modelling system ran in a cluster installed at the Servicio Meteorológico Nacional (SMN) of Argentina with funds from the Argentinean Project PIDDEF 41/10: “Pronóstico del tiempo para estudios de vulnerabilidad e impacto socioeconómico”, which also

supported partly this research and M. E. Dillon fellowship (2010-2012). The observational dataset was provided by the SMN.

The GLDAS data used in this study were acquired as part of the mission of NASA's Earth Science Division and archived and distributed by the Goddard Earth Sciences (GES) Data and Information Services Center (DISC).

References

Angelini, I.M., Garstang, M., Davis, R.E., Hayden, B., Fitzjarrald, D.R., Legates, D.R., Greco, S., Macko, S., Connors, V., 2011. On the coupling between vegetation and the atmosphere. Theor. Appl. Climatol. 105, 243–261. http://dx.doi.org/10.1007/s00704-010-0377-5.

Arndt, D.S., Baringer, M.O., Johnson, M.R., 2010. State of the climate in 2009. BAMS 91 (7), s1–s222.

Berbery, H., et al., 2014. The Joint Assessment of Soil Moisture Indicators Project. A community effort to respond to users needs in agriculture and water resources. Satellite Soil moisture validation & application workshop, Amsterdam, The Netherlands, 10-11 July 2014 (http://www.hydrology-amsterdam.nl/SoilMoistureWS_Adam14/PostersAndPresentations/Berbery_presentation.pdf).

Berbery, E.H., Collini, E.A., 2000. Springtime precipitation and water vapor flux over Southeastern South America. Mon. Weather Rev. 128, 1328–1346.

Berbery, E.H., Rasmusson, E.M., 1999. Mississippi moisture budgets on regional scales. Mon. Weather Rev. 127, 2654–2673.

Betts, A.K., 2009. Land-surface-atmosphere coupling in observations and models. J. Adv. Model. Earth Syst. 1. http://dx.doi.org/10.3894/JAMES.2009.1.4.

Betts, A.K., Viterbo, P., 2005. Land-surface, boundary layer, and cloud-field coupling over the southwestern Amazon in ERA-40. J. Geophys. Res. 110, D14108. http://dx.doi.org/10.1029/2004JD005702.

Betts, A.K., Miller, M.J., 1986. A new convective adjustment scheme. Part II: single column tests using GATE wave, BOMEX, ATEX and Artic air-mass data sets. Q. J. R. Meteorol. Soc. 112, 693–710.

Cavalcanti, I.F.A., et al., 2002. Global climatological features in a simulation using the CPTEC-COLA AGCM. J. Clim. 15, 2965–2988.

Chen, F., Dudhia, J., 2001. Coupling an advanced land-surface/hydrology model with the Penn State/ NCAR MM5 modeling system. Part I: Model description and implementation. Mon. Weather Rev. 129, 569–585.

Chen, F., Janjic, Z.I., Mitchell, K.E., 1997. Impact of atmospheric surface layer parameterization in the new land-surface scheme of the NCEP Mesoscale Eta Numerical Model. Bound.-Layer Meteorol. 85, 391–421.

Collini, E.A., Ferreira, L., Dillon, M.E., Osores, S., Pujol, G., Martin, P., Suaya, M., Folch, A., 2011. Different Aspects of WRF-ARW applications at the National Meteorological Service – and Naval Hydrographic Service of Argentina. WGNE Blue Book 2011 (http://www.wcrp-climate.org/WGNE/BlueBook/2011/individual-articles/05_Collini_Estela__Collini_etal_bluebook_2011.pdf).

Collini, E.A., Berbery, E.H., Barros, V., 2008. How Does Soil Moisture Influence the Early Stages of the South American Monsoon? J. Clim. 21, 195–213.

De Goncalves, L.G.G., Shuttleworth, W.J., Chou, S.C., Xue, Y., Houser, P.R., Toll, D.L., Marengo, J., Rodell, M., 2006. Impact of different initial soil moisture fields on Eta model weather forecasts for South America. J. Geophys. Res. 111. http://dx.doi.org/10.1029/2005JD006309 D17102.

Dillon, M.E., Collini, E.A., Ferreira, L., Pujol, G., Dadamia, D., 2012. Comparación entre los datos de humedad de suelo obtenidos en campañas de medición y los resultados de modelos globales de suelo y estimaciones de sensores remotos. IFRH 14-15 June 2012, Ezeiza, Argentina (http://www.ina.gov.ar/pdf/ifrrhh/03_007_Dillon.pdf).

Dillon, M.E., Ferreira, L., Collini, E.A., Pujol, G., 2011. Estudio de la sensibilidad del modelo WRF-ARW versión SMN/SHN usando campos de humedad del suelo del GLDAS. Conferencia Geográfica Regional, UGI, 14-18 November 2011, Chile.

Dirmeyer, P.A., Jin, Y., Singh, B., Yan, X., 2013. Trends in Land–Atmosphere Interactions from CMIP5 Simulations. J. Hydrometeorol. 14, 829–849. http://dx.doi.org/10.1175/JHM-D-12-0107.1.

Dirmeyer, P.A., Cash, B.A., Kinter III, J.L., Stan, C., Jung, T., Marx, L., Towers, P., Wedi, N., Adams, J.M., Altshuler, E.L., Huang, B., Jin, E.K., Manganello, J., 2012. Evidence for Enhanced Land–Atmosphere Feedback in a Warming Climate. J. Hydrometeorol. 13, 981–995. http://dx.doi.org/10.1175/JHM-D-11-0104.1.

Dirmeyer, P.A., Schlosser, C.A., Brubaker, K.L., 2009. Precipitation, Recycling, and Land Memory: An Integrated Analysis. J. Hydrometeorol. 10, 278–288.

Dirmeyer, P.A., Guo, Z., Gao, X., 2004. Comparison, validation and transferability of eight multi-year global soil wetness products. J. Hydrometeorol. 5, 1011–1033.

Dorigo, W.A., Wagner, W., Hohensinn, R., Hahn, S., Paulik, C., Xaver, A., Gruber, A., Drusch, M., Mecklenburg, S., van Oevelen, P., Robock, A., Jackson, T., 2011. The international soil moisture network: a data hosting facility for global in situ soil moisture measurements. Hydrol. Earth Syst. Sci. 15, 1675–1698.

Draper, C.S., Walker, J.P., Steinle, P.J., de Jeu, R.A.M., Holmes, T.R.H., 2009. An evaluation of AMSR-E derived soil moisture over Australia. Remote Sens. Environ. 113, 703–710.

Dudhia, J., 1989. Numerical study of convection observed during the winter monsoon experiment using a mesoscale two-dimensional model. J. Atmos. Sci. 46, 3077–3107.

Eltahir, E.A.B., 1998. A soil moisture-rainfall feedback mechanism: 1. Theory and observations. Water Resour. Res. 34, 765–776.

Ferguson, C.R., Wood, E.F., Vinukollu, R.K., 2012. A Global Intercomparison of Modeled and Observed Land–Atmosphere Coupling. J. Hydrometeorol. 13, 749–784. http://dx.doi.org/10.1175/JHM-D-11-0119.1.

Ferreira, L., Salgado, H., Saulo, C., Collini, E.A., 2011. Comparison of soil moisture values derived from models with observations from a field campaign over Argentina. Atmos. Sci. Lett. 12 (4), 334–339.

Grimm, A., Pal, J.S., Giorgi, F., 2007. Connection between Spring Conditions and Peak Summer Monsoon Rainfall in South America: Role of Soil Moisture, Surface Temperature, and Topography in Eastern Brazil. J. Clim. 20, 5929–5945.

Hillel, D., 1998. Environmental soil physics. Academic Press, Elsevier (771 pp.).

Hirsch, A.L., Pitman, A.J., Kala, J., 2014. The role of land cover change in modulating the soil moisture-temperature land-atmosphere coupling strength over Australia. Geophys. Res. Lett. 41 (16), 5883–5890. http://dx.doi.org/10.1002/2014GL061179.

Janjic, Z.I., 2002. Nonsingular Implementation of the Mellor–Yamada Level 2.5 Scheme in the NCEP Meso model. NCEP Office Note 437 (61 pp.).

Janjic, Z.I., 1996. The surface layer in the NCEP Eta Model. Eleventh Conference on Numerical Weather Prediction, Norfolk, VA, 19–23 August. Amer. Meteor. Soc., Boston, MA, pp. 354–355.

Janjic, Z., 1994. The step-mountain Eta coordinate: further developments of the convection, viscous sublayer, and turbulence closure schemes. Mon. Weather Rev. 122, 927–945.

Janjic, Z., 1990. The step-mountain coordinate physical package. Mon. Weather Rev. 118, 1429–1443.

Koren, V., Schaake, J., Mitchell, K., Duan, Q.Y., Chen, F., Baker, J.M., 1999. A parameterization of snowpack and frozen ground intended for NCEP weather and climate models. J. Geophys. Res. 104, 19569–19585.

Koster, R.D., Zhichang, G., Rongqian, Y., Dirmeyer, P., Kenneth, M., Puma, M., 2009. On the Nature of Soil Moisture in Land Surface Models. J. Clim. 22, 4322–4335.

Koster, R.D., et al., 2004. Regions of strong coupling between soil moisture and precipitation. Science 305, 1138–1140. http://dx.doi.org/10.1126/science.1100217.

Koster, R.D., Suarez, M.J., 1996. The influence of land surface moisture retention on precipitation statistics. J. Clim. 9, 2551–2567.

Liang, X., Lettenmaier, D.P., Wood, E.F., 1996. One-dimensional Statistical Dynamic Representation of Subgrid Spatial Variability of Precipitation in the Two-Layer Variable Infiltration Capacity Model. J. Geophys. Res. 101 (D16), 21,403–21,422.

Liang, X., Lettenmaier, D.P., Wood, E.F., Burges, S.J., 1994. A Simple hydrologically Based Model of Land Surface Water and Energy Fluxes for GSMs. J. Geophys. Res. 99 (D7), 14,415–14,428.

Liu, Y.Y., McCabe, M.F., Evans, J.P., van Dijk, A.I.J.M., de Jeu, R.A.M., Su, H., 2009. Comparison of soil moisture in GLDAS model simulations and satellite observations over the Murray Darling Basin. The 18th World IMACS Congress and MODSIM09 International Congress on Modelling and Simulation. Cairns, Australia, pp. 2798–2804.

Mellor, G.L., Yamada, T., 1982. Development of a turbulence closure model for geophysical fluid problems. Rev. Geophys. Space Phys. 20, 851–875.

Miguez-Macho, G., Li, H., Fan, Y., 2008. Simulated water table and soil moisture climatology over North America. Bull. Am. Meteorol. Soc. 5, 663–672.

Mlawer, E.J., Taubman, S.J., Brown, P.D., Iacono, M.J., Clough, S.A., 1997. Radiative trans-fer for inhomogeneous atmosphere: RRTM, a validated correlated-k model for the longwave. J. Geophys. Res. 102, 16663–16682.

Monin, A.S., Obukhov, A.M., 1954. Basic laws of turbulent mixing in the surface layer of the atmosphere. Contrib. Geophys. Inst. Acad. Sci. USSR (151), 163–187 (in Russian).

Njoku, E., 1999. AMSR Land Surface Parameters. Algorithm Theoretical Basis Document: Surface Soil Moisture, Land Surface Temperature, Vegetation Water Content, Version 3.0. NASA Jet Propulsion Laboratory, Pasadena, California USA.

Owe, M., de Jeu, R.A.M., Colmes, T., 2008. Multi-Sensor Historical Climatology of Satellite-Derived Global Land Surface Moisture. J. Geophys. Res. 113, F01002. http://dx.doi.org/10.1029/2007JF000769.

Pal, J.S., Eltahir, E.A.B., 2003. A feedback mechanism between soil-moisture distribution storm tracks. Q. J. R. Meteorol. Soc. 129, 1–19.

Pathirana, A., Denekew, H.B., Veerbeek, W., Zevenbergen, C., Banda, A.T., 2014. Impact of urban growth-driven landuse change on microclimate and extreme precipitation – A sensitivity study. Atmos. Res. 138, 59–72. http://dx.doi.org/10.1016/j.atmosres.2013.10.005.

Peterson, T.C., Baringer, M.O., 2009. State of the climate in 2008. Bull. Am. Meteorol. Soc. 90 (8), s1–s196.

Rodell, M., Houser, P.R., Jambor, U., Gottschalck, J., Mitchell, K., Meng, C.J., Arsenault, K., Cosgrove, B., Radakovich, J., Bosilovich, M., Entin, J.K., Walker, J.P., Lohmann, D., Toll, D., 2004. The Global Land Data Assimilation System. Bull. Am. Meteorol. Soc. 85, 381–394.

Rudiger, C., Calvet, J., Gruhier, C., Holmes, T.R.H., de Jeu, R.A.M., Wagner, W., 2009. An intercomparison of ERS-Scat and AMSR-E Soil Moisture Observations with Model Simulations over France. J. Hydrometeorol. 10, 431–447.

Rui, 2011. README Document for Global Land Data Assimilation System Version 1 (GLDAS-1) Products. Goddard Earth Sciences, Data and Information Services Center, National Aeronautics and Space Administration.

Ruiz, J., Saulo, C., Nogués-Paegle, J., 2010. WRF Model sensitivity to choice of parametrization over South America: Evaluation against surface observation. Mon. Weather Rev. 138, 3342–3355.

Ruscica, R.C., Sörensson, A.A., Menéndez, C.G., 2014. Pathways between soil moisture and precipitation in southeastern South America. Atmos. Sci. Lett. http://dx.doi.org/10.1002/asl2.552.

Saha, Suranjana, et al., 2010. The NCEP Climate Forecast System Reanalysis. Bull. Am. Meteorol. Soc. 91, 1015–1057.

Sánchez-Mejía, Zulia M., 2013. Monsoon dependent ecosystems: implications of the vertical distribution of soil moisture on land surface-atmosphere interactions. http://cals.arizona.edu/research/papuga/docs/SanchezMejiaDissertation.pdf.

Santanello Jr., J.A., Peters-Lidard, C.D., Kennedy, A., Kumar, S.V., 2013. Diagnosing the Nature of Land–Atmosphere Coupling: A Case Study of Dry/Wet Extremes in the

U.S. Southern Great Plains. J. Hydrometeorol. 14, 3–24. http://dx.doi.org/10.1175/JHM-D-12-023.1.

Saulo, C., Ferreira, L., Pages, J., Seluchi, M., Ruiz, J., 2010. Land-atmosphere interactions during a Northwestern Argentina Low event. Mon. Weather Rev. 138, 2481–2498.

Seneviratne, S.I., Corti, T., Davin, E.L., Hirschi, M., Jaeger, E.B., Lehner, I., Orlowsky, B., Teuling, A.J., 2010. Investigating soil moisture-climate interactions in a changing climate: A review. Earth Sci. Rev. 99, 125–161. http://dx.doi.org/10.1016/j.earscirev.2010.02.004.

Seth, A., Rojas, M., 2003. Simulation and sensitivity in a nested modeling system for tropical South America. Part I: Reanalyses boundary forcing. J. Clim. 16, 2437–2453.

Sörensson, A.C., Menéndez, G., Samuelsson, P., Willén, U., Hansson, U., 2010. Soil-precipitation feedbacks during the South American Monsoon as simulated by a regional climate model. Clim. Chang. 98, 429–447. http://dx.doi.org/10.1007/s10584-009-9740-x.

Spennemann, Pablo, 2010. Evaluación de la representación de la humedad de suelo por el modelo WRF-ARW (Graduate Thesis) Department of Atmospheric and Oceanic Sciences, University of Buenos Aires.

Su, F., Hong, Y., Lettenmaier, D.P., 2008. Evaluation of TRMM Multisatellite Precipitation Analysis (TMPA) and its utility in hydrologic prediction in the La Plata Basin. J. Hydrometeorol. 9, 622–640.

Wei, J., Dirmeyer, P.A., 2012. Dissecting soil moisture – precipitation coupling. Geophys. Res. Lett. http://dx.doi.org/10.1029/2012GL053038.

Yilmaz, K.K., Hogue, T.S., Hsu, K.-L., Sorooshian, S., Gupta, H.V., Wagener, T., 2005. Intercomparison of rain gauge, radar, and satellite-based precipitation estimates with emphasis on hydrologic forecasting. J. Hydrometeorol. 6, 497–517.

Zaitchik, B.F., Santanello, J.A., Kumar, S.V., Peters-Lidard, C.D., 2013. Representation of Soil Moisture Feedbacks during Drought in NASA Unified WRF (NU-WRF). J. Hydrometeorol. 14, 360–367. http://dx.doi.org/10.1175/JHM-D-12-069.1.

Zhang, J., Wang, W., Wei, J., 2008. Assesing land-atmosphere coupling using soil moisture from the Global Land Data Assimilation System and observational precipitation. J. Geophys. Res. 113, 14. http://dx.doi.org/10.1029/2008JD009807.

Zhao, Q., Carr, F.H., 1997. A prognostic cloud scheme for operational NWP models. Mon. Weather Rev. 125, 1931–1953.

Zilitinkevich, S.S., 1995. Non-local turbulent transport: pollution dispersion aspects of coherent structure of convective flows, Air Pollution III — Volume I. In: Power, H., Moussiopoulos, N., Brebbia, C.A. (Eds.), Air Pollution Theory and Simulation. Computational Mechanics Publications, Southampton Boston, pp. 53–60.